

UC Berkeley

UC Berkeley Previously Published Works

Title

Chapter Nine Monitoring neuronal activity with voltage-sensitive fluorophores

Permalink

<https://escholarship.org/uc/item/0ch9j61k>

ISBN

9780128211533

Authors

Kirk, Molly J
Raliski, Benjamin K
Miller, Evan W

Publication Date

2020

DOI

10.1016/bs.mie.2020.04.028

Peer reviewed



Published in final edited form as:

Methods Enzymol. 2020 ; 640: 185–204. doi:10.1016/bs.mie.2020.04.028.

Monitoring neuronal activity with voltage-sensitive fluorophores

Molly J. Kirk^a, Benjamin K. Raliski^b, Evan W. Miller^{a,b,c,*}

^aDepartment of Molecular and Cell Biology, University of California, Berkeley, CA, United States

^bDepartment of Chemistry, University of California, Berkeley, CA, United States

^cHelen Wills Neuroscience Institute, University of California, Berkeley, CA, United States

Abstract

Voltage imaging in living cells offers the tantalizing possibility of combining the temporal resolution of electrode-based methods with the spatial resolution of imaging techniques. Our lab has been developing voltage-sensitive fluorophores, or VoltageFluors, that respond to changes in cellular and neuronal membrane potential via a photoinduced electron transfer (PeT)-based mechanism. This unique mechanism enables both the fast response kinetics and high sensitivity required to record action potentials in single trials, across multiple cells without the need for stimuli-triggered averaging.

In this chapter, we present a methodology for imaging membrane potential dynamics from dozens of neurons simultaneously *in vitro*. Using simple, commercially available cameras, illumination sources, and microscope optics in combination with the far-red synthetic voltage-sensitive fluorophore BeRST-1 (Berkeley Red Sensor of Transmembrane potential) provides a readily applied method for monitoring neuronal activity in cultured neurons. We discuss different types of voltage-sensitive dyes, considerations for selecting imaging modalities, and outline procedures for the culture of rat hippocampal neurons and performing voltage imaging experiments with these samples. Finally, we provide an example of how changes to the metabolic input to cultured hippocampal neurons can alter their activity profile.

1. Introduction

Action potentials are the basis of neural signaling. These rapid changes in membrane potential underlie the vast array of computations, perceptions, and outputs of the human brain. Disruption to the coordinated firing of neurons within the brain has profound detrimental effects on human health. For example, epilepsy is characterized by excessive rhythmic activity of susceptible neuronal populations and can result in hyperexcitability and excitotoxic death in affected neural circuits (Kawamura, Ruskin, & Masino, 2016). In order to prevent such outcomes, neuronal activity is highly regulated by circuit-based feedback mechanisms, intracellular signaling pathways, and the overall metabolic state of the cell. To obtain deeper insight into neuronal activity and its regulation, it is required to monitor activity while simultaneously perturbing these relevant regulatory systems.

*Corresponding author: evanwmiller@berkeley.edu.

To this end, many techniques have been developed to record action potentials in a high throughput manner. Multi-electrode arrays (MEA), for example, record the activity of large populations of neurons via extracellular electrodes with excellent temporal resolution (Pine, 2006). However, this technique lacks spatial resolution. It records the local field potential and local spike activity but gives little information about which specific neuron exhibited which electrical activity. Calcium imaging, on the other hand, can be used to record from large numbers of neurons simultaneously with both genetic and spatial specificity (Chen et al., 2013; Scanziani & Häusser, 2009; Sofroniew, Flickinger, King, & Svoboda, 2016). However, calcium imaging measures a secondary response to action potentials, which is an order of magnitude slower than the electrical signal and is liable to confounds such as calcium release from internal stores. An attractive alternative to these two approaches is voltage imaging, which combines the spatial resolution of an imaging technique with the temporal resolution and direct measurement of electrode recordings.

In this chapter, we will discuss the use of voltage-sensitive fluorophores for directly imaging voltage changes in neurons *in vitro*. We provide an overview of voltage-sensing approaches and introduce our method of monitoring voltage changes via indicators that we propose operate via a photoinduced electron transfer (PeT) method (Fig. 1A). We then discuss considerations for performing voltage imaging, including methods of detection and choice of filter sets.

To illustrate the PeT voltage-sensitive dye imaging technique, we will explore the effect of the cellular metabolic state on neuronal firing rate. Recent studies have shown that switching the fuel source from glucose to ketone body β -hydroxybutyrate (β HB) causes a dramatic decrease in neuronal activity, which is mediated by the opening of K-ATP channel (Ma, Berg, & Yellen, 2007; Sada, Lee, Katsu, Otsuki, & Inoue, 2015). The K-ATP channel conducts a large potassium selective current, and its open probability is gated by the absence of adenosine triphosphate (ATP). This leads ultimately to a decrease in neuronal activity during times of starvation (Roepert, 2001). Using β -hydroxybutyrate as a model for pharmacological perturbations of neuronal activity, we will describe how to use voltage-sensitive dyes to monitor neuronal activity and its perturbations from a mechanistic perspective.

2. Voltage imaging with voltage-sensitive fluorophores

Voltage imaging emerged as a method with the discovery of voltage-sensitive dyes. Synthetic voltage indicators have traditionally been divided into two classes: electrochromic (fast) voltage-sensitive dyes, and Nernstian (slow) voltage-sensitive dyes. Electrochromic dyes show sub-millisecond temporal resolution but exhibit extremely small signal amplitudes. Slow voltage-sensitive dyes, on the other hand, have a greater fractional fluorescence change per millivolt but exhibit slow dynamics, as well as capacitive loading. For a more comprehensive review of voltage-sensitive dyes, we direct readers to previous reviews on the subject (Braubach, Cohen, & Choi, 2015; Miller et al., 2012).

Our group has initiated a program to develop synthetic voltage-sensitive indicators that can provide large changes in fluorescence in response to membrane potential changes while

maintaining the rapid response kinetics needed to monitor action potentials in a single trial (Liu & Miller, 2020). We hypothesize that PeT-based voltage-sensitive fluorophores utilize a photoinduced electron transfer mechanism to sense the potential difference across the membrane (Fig. 1A). At rest, PeT holds the fluorophore in a quenched state, but upon depolarization, the rate of electron transfer is diminished, and the fluorophore becomes unquenched and bright. This results in an increased fluorescence in response to neuronal activity (Fig. 1A). Ultimately, PeT-based voltage-sensitive dyes are a noninvasive and readily applicable method for monitoring neuronal activity in vitro. A number of voltage-sensitive fluorophores, or VoltageFluors, are available in a range of wavelengths spanning most of the visible spectrum (Fig. 1B).

Despite the recent emergence of a variety of genetically encoded and genetically-encoded/small molecule hybrid voltage indicators (Abdelfattah et al., 2019; Lin & Schnitzer, 2016), voltage-sensitive dyes remain one of the most commonly used methods for in vitro studies of neuronal activity. This is in part because they do not require genetic transfection or transduction and thus are readily applicable to any culture of interest—especially those model systems without a well-developed complement of genetic tools (Tomina & Wagenaar, 2017). Because the PeT-based VoltageFluor-style indicators developed in our lab maintain rapid response kinetics and high signal to noise ratios, they are a powerful method for monitoring neuronal activity in vitro.

2.1 Challenges and pitfalls often encountered in voltage imaging

Voltage imaging has been a long-standing goal in the neuroscience community, yet has remained difficult to implement compared to techniques such as calcium imaging (Kulkarni & Miller, 2017). This is in part due to the complex challenges of acquiring, detecting and processing voltage imaging data. This section will directly address the challenges often encountered when using this technique and demonstrate how to resolve them in functional imaging studies.

2.2 Detector selection and sampling rates

A critical challenge in the application of voltage imaging is obtaining sufficient temporal resolution to detect action potentials while simultaneously collecting enough photons to resolve signals from noise (Sjulson & Miesenböck, 2007). This balancing act depends on the type of experiments in question, but some overarching principles can be useful for determining the optimal sampling rate. According to Nyquist sampling theory, to accurately detect events within a signal, one must sample at a rate two times faster than the fastest event (Craven, McGinley, Kilmartin, Glavin, & Jones, 2015; Sjulson & Miesenböck, 2007). This would require a 1–2kHz sampling rate to reliably detect action potentials with their characteristic 1–2ms duration.

For the protocols described here, we are concerned with detecting spikes across multiple neurons. A sampling rate of 500Hz represents a reasonable compromise between spike detection and photon collection. Under-sampling at 500Hz increases photon integration time and improves the spike detection by enhancing the signal-to-noise ratio (SNR), thus permitting high fidelity action potential detection. Although under-sampling is acceptable

for spike detection, the data shows mild aliasing, which can result in variations in spike height. For this reason, if the aim is to collect data concerning spike amplitude, waveform characteristics, or rise and decay kinetics, higher sampling rates may be required.

To achieve the high sampling rates required by voltage imaging, we find it most convenient to utilize standard wide-field epifluorescence microscopy with LED illumination. Although functional imaging methods like Ca^{2+} imaging often rely on confocal or two-photon (2P) microscopy, for voltage imaging, these raster scanning microscopies cannot achieve fast frame rates. Due to these limitations, the current standard for imaging of voltage transients is wide-field epifluorescence coupled with a cooled fast EMCCD or CMOS camera. This allows for rapid acquisition of data with commercially available components, although new methods are improving the frame rates that can be obtained using 2P illumination (Kazempour et al., 2019; Wu et al., 2020).

2.3 Maintenance of cell health prevents unwanted erosion of SNR

Voltage imaging is a highly photon-limited imaging modality. A number of factors influence the scarcity of photons for voltage imaging (Kulkarni & Miller, 2017). First, the event kinetics of action potentials are at least an order of magnitude faster than transient increases in cytosolic Ca^{2+} . Second, for voltage imaging, only dye that is properly localized to the cellular membrane actually reports voltage changes. As a result, compared to cytosolic Ca^{2+} indicators, there is a small pool of voltage indicators that can contribute to the voltage-sensitive fluorescence response. This restriction requires that the fractional change in fluorescence and brightness of each molecule be very large in comparison to a cytosolic indicator, whose bulk concentration can overcome a smaller fractional change. Any dye molecule not localized to the extracellular surface will erode the SNR by increasing the background of the sample. PeT-based voltage indicators localize to the plasma membrane of healthy cells. In contrast, unhealthy and dying cells take up PeT voltage-sensitive dyes, resulting in cytosolic labeling, dramatically increasing the background. For this reason, controlling cell health and integrity throughout an experiment is crucial. To maintain cellular health and prevent dye internalization, we keep neuron cultures at 37°C and 5% CO_2 until immediately before imaging. This preserves the integrity of the cells and allows for extended imaging of neuronal activity. Heated and oxygenated stage inserts may also improve cell health, but we have not found them necessary for experimental success. We next turn our attention to the neuron cultures.

3. Primary hippocampal cell culture

We have optimized a cell culture protocol for primary hippocampal neuron preparation, which both minimizes variability when performed in a stereotyped manner and maintains the sample under metabolically relevant conditions. To this end, we used BrainPhys as our culture media for these experiments. BrainPhys mimics physiologically relevant glucose levels found in the brain: 2.5mM glucose as opposed to the 10–25mM glucose found in most neuronal media (Bardy et al., 2015). It should be noted, however, that if your experiment does not depend on the metabolic state of the cell, you can also use Neurobasal media with little effect on neuronal health or activity.

Finally, controlling for variation is of utmost importance to reduce variability in cell health. Small variations in cell density and dissection quality can affect the basal activity rates of the cultured neurons. As a result, we have found it useful to have one or two members of our lab perform the dissections and culturing for all of our experiments to reduce individual variation between preps. When this protocol is performed in a very standardized manner, it will permit stable, reproducible recordings over multiple preparations.

3.1 Materials

0.2µm sterile filter, 50 mL (VWR 82027-592)

Cell culture plates 24 wells (VWR 62406-183)

12mm round German glass coverslips (VWR 100499-634)

Glass petri dishes (VWR 75845-542)

Synergy Water Purification System (Millipore Sigma Synergy W-R)

General purpose heating and drying oven (Fisher Scientific 15-103-0503)

Incubator (ThermoFisher Scientific Heracell VIOS 160i)

Dissection microscope (Olympus SZ40 Stereo Zoom)

Tissue culture hood (Baker SterilGARD e3)

Forceps, Dumont #5 for rat dissection, fine tips (Fine Science Tools 11251-20)

Scissors, curved, for rat dissection (VWR 25608-225).

Dissecting Scissors, Sharp Tip, 6 1/2" (VWR 82027-592)

Positive action tweezers, Style 5 (Electron Microscopy Services 72706-01)

50mL centrifuge tubes, Corning (VWR 21008-725)

15mL centrifuge tubes, Corning (VWR 21008-673)

Aspirator pipettes 2mL, Falcon (VWR 53106-450)

Serological pipettes, 1mL (VWR 29443-041)

Pipets, serological, 5mL (VWR 29443-045)

Pipets, serological, 10mL (VWR 29443-047)

Pasteur pipets (FisherScientific 13-678-20C)

Hemocytometer (VWR 15170-089).

3.2 Reagents

Hydrochloric acid (CAS; 7647-01-0)

Ethanol (CAS: 64-17-5)

Sodium Borate Buffer (PB, see recipe in Section 7)

Poly-D-Lysine (Sigma-Aldrich P7280—5mg)

Culture media MEM++++ (see recipe in Section 7)

Brain Phys media (see recipe in Section 7)

Calcium/Magnesium Free Hanks Balanced Salt Solution with Phenol

Red (HBSS, Invitrogen 14170-16)

Dulbecco's phosphate buffered saline (DPBS, Gibco 14200-075)

Timed pregnant Sprague Dawley rat (Charles River Laboratories)

Trypsin, 2.5%, for neuron dissection (Invitrogen 15090-046)

3.2.1 Optional—Neurobasal media++ (see recipe in Section 7).

3.3 Protocol for primary culture

1. 2 weeks prior to dissection, acid wash 12mm coverslips to prepare and sterilize the plating surface.
 - a. Place 12mm coverslips in a clean glass petri dish and cover with a solution of 1M HCl. Shake at 90 RPM for 3–5h at room temperature.

All wash steps throughout the protocol are performed at room temperature.
 - b. Remove the acid solution and replace it with 100% ethanol shaking at 100 RPM overnight. Wash two more times for a total of three overnight washes.
 - c. Remove the final ethanol wash and replace it with double distilled water. Wash a total of three times overnight at 100 RPM.
 - d. Remove the water and place the dish into a glassware oven (150°C) for 2–5h or until completely dry. Once these cool, you can store them at room temperature and use them as needed.

To maintain sterility, we have found it best to leave the cleaned coverslips in the petri dish with the lid sealed with parafilm or taped shut to prevent accidental contamination.

2. 1 day prior to tissue collection, make a fresh 1:10 dilution of PDL (stock: 1mg/mL in PB) in sterile DPBS.
Final concentration is 0.1mg/mL PDL.
3. Using sterile forceps, place acid-washed coverslips into the tissue culture plate and cover each coverslip with the PDL solution incubating them overnight at 37°C in a culture incubator.
For a 24 well plate containing 12mm coverslips, we use 250µL per well to ensure even coating of the glass.
4. On the day of the prep, aspirate the PDL. Wash two times with sterile double distilled water and two times with sterile DPBS.
5. Add half of the plating volume (400µL per 24 well) of MEM++++ to each well and allow the plate to equilibrate to the CO₂ in the incubator.
For 24 well plates 12mm coverslips we plate in a total volume of 750µL per well, adding 400µL for equilibration and 350µL for plating cells.
6. Euthanize a timed pregnant female Sprague Dawley rat at E17–19 in accordance with IACUC approved protocols.
7. Make a caudal to rostral cut along the ventral side of the abdomen, remove the embryonic sac and subsequently, the embryos. Decapitate the embryos using sterile technique and place the heads in ice-cold HBSS.
8. Puncture through the most rostral portion of the cranium with fine forceps. In a rostral to caudal fashion, remove skin and skull cutting along the longitudinal fissure using forceps or scissors. Pull away the remaining skull and meninges using fine forceps, being careful not to puncture or damage the brain as you extract it. Bisecting the brain along the longitudinal fissure, expose the hippocampi on either side and dissect them away using fine forceps. Place them into fresh ice-cold HBSS. Discard all carcasses, blood, and tissue as medical waste in accordance with regulations.
For more details see Fig. 2 and Audesirk, Audesirk, and Ferguson (2000).
9. Transfer the hippocampi to 1mL of 2.5% trypsin and incubate for 15min at 37°C.
10. Remove the trypsin and wash hippocampi three times in fresh HBSS, being careful each time not to aspirate the tissue. Finally, replace the media with 1mL of MEM++++.
11. Triturate three times with increasingly smaller flame polished sterile glass pipettes until the solution appears homogenous and then add 2mL of MEM++++.
12. Measure cell density using a hemocytometer and plate neurons onto the equilibrated dish at the appropriate density.
30,000 cells per 12mm coverslip in a 24 well plate is a good density for most functional imaging experiments.

13. At 1 day in vitro (DIV), change half of the plating media to Brain Phys++ media and at 7 DIV, add 500 μ L of Brain Phys++ media to the cells.

4. Functional voltage imaging of cultured neurons

We have established a functional imaging protocol that allows recording of action potentials and subsequent calculation of firing frequency in dissociated hippocampal cultures under varying conditions. First, select healthy cultures aged 14–16 DIV, this is done to ensure that the neurons will fire action potentials, have developed fully functioning synapses, and have integrated into circuits. Cells are then loaded for 30min with 500nM Berkeley Red Sensor of Transmembrane potential (BeRST1), a far-red PeT voltage-sensitive dye that is excited at 658nm and emits at 683nm. Due to the photon starved nature of voltage imaging, it is important to select filters and dichroic mirrors which permit the on-peak excitation and collection of fluorescent signals. Near-optimal filter sets and dichroics are shown in (Fig. 2A); filter sets optimized for Cy5 are usually fairly close to optimal for BeRST imaging. This technique is amenable for use with any of the PeT-based VoltageFluors (Deal et al., 2020; Miller et al., 2012; Ortiz, Liu, Naing, Muller, & Miller, 2019), but BeRST 1 was selected for its photostability and robust SNR (Huang, Walker, & Miller, 2015).

The cells are then transferred to the microscope, and a field of view (FOV) containing healthy cells (Fig. 2B and C) is selected via differential interference microscopy (DIC) or brightfield imaging. In order to assess cell health, we suggest looking for four different characteristics: an even dispersion of cells lacking neurosphere formation (Fig. 2D), a lack of blebbing on the plasma membrane (Fig. 2E), a distinct nucleus in large diameter cells (Fig. 2F), and lack of dye internalization (Fig. 2G). These are outlined visually in Fig. 2B–G. Once having selected a region of interest for imaging, focus the sample under fluorescent light and begin recording. Two 10s recordings are taken per field of view and 4 fields are taken per sample to allow for detection of unhealthy cells and outlier data points. Overall, recording should take less than 20min per sample, permitting rapid data acquisition and preventing the deterioration of cell health by minimizing exposure to light and ambient temperature. The protocol below outlines (1) software and hardware configuration for fast, functional imaging, (2) functional imaging protocol for single perturbations and (3) functional imaging protocols for repeat measures in both pretreatment and rescue experiments.

4.1 Materials

- 50mL centrifuge tubes, Corning (VWR 21008-725)
- Aspirator pipettes 2mL, Falcon (VWR 53106-450)
- 0.2 μ m Sterile filter, 50mL (VWR 82027-592) 50mL falcon tubes
- Incubator (ThermoFisher Scientific Heracell VIOS 160i)
- Fine Forceps #5 (Fine Science Tools 11251-20)
- 1.5 Eppendorf tubes (Fisher Scientific 14222155)

Imaging Chamber (Warner RC-26 or VWR 25382-348)

Inverted or upright epifluorescence microscope (AxioExaminer Z-1 Zeiss)

20× Objective

Filter set compatible with BeRST1 spectrum

LED or Epifluorescence lamp

Dichroic compatible with filter sets for BeRST1

Fast sCMOS or EMCCD camera (Orca Flash 4.0 v2, Hamamatsu)

Software to control image capture (we have used both MicroManger and Slidebook)

4.1.1 Optional—Gridded coverslip.

4.2 Reagents

BeRST dye (250 μ M in DMSO, available from the corresponding author upon request)

Metabolic Saline Solution (MSS, see recipe in Section 7)

Day 14–16 DIV dissociated cultures

4.2.1 Optional—If cultures are maintained in Neurobasal, we suggest using HBSS as an imaging solution to maintain similar levels of glucose between culture conditions and imaging conditions.

Calcium/Magnesium Free Hanks Balanced Salt Solution without Phenol Red (HBSS, Invitrogen 14170-16).

4.3 Detector configuration

1. See that the computer has been recently restarted and has plenty of space on the hard drive. This will ensure that the rate of data acquisition will not be slowed down by storage constraints.

Tip: If the acquisition rate decreases throughout a recording, hard drive space is often the issue. We have found it optimal to have two times as much space on the hard drive as the data to be collected.

2. Select an imaging field of view (FOV) that is centered at the chip read-out point for your camera. The largest FOV on the Orca Flash 4.0-v2 (Hamamatsu) is 2048 \times 400 pixels.
3. Determine the minimum binning permitted while maintaining fidelity and speed of FOV acquisition.

We have found that 4 \times 4 binning resulting in a 512 \times 100 pixel FOV is optimal for the Orca Flash 4.0, but you will need to determine the binning value

empirically for each different detector by referring to the metadata frame rate and number of frames.

Finally, if possible, stream data acquisition directly to the disk, this protects against dropped frames or slowing as your data size increases.

4. Once the acquisition has been fully optimized, acquire two 10s test videos and verify via frame rate and number of frames that the detector accurately tracks at 500Hz. The optimization of your imaging FOV should only need to be performed once and can be reused for future experiments.

4.4 Functional imaging and data acquisition

1. At 14–16 DIV cells are ready to perform functional imaging.
2. Warm the imaging solutions to 37°C prior to beginning the experiment to prevent temperature shock to the cells.
3. Take 1µL of 250µM BeRST1 solution and dilute it to 500nM in 499µL of MSS solution containing pharmacological agent or vehicle control. Mix thoroughly.
4. Gently, aspirate the media from one well and replace it with the dye solution. Return the culture plate immediately to the incubator and incubate for 30min.

Depending on the drug/perturbation time course, this incubation period may vary. However, around 20min provides good membrane staining of neurons. Longer incubation times are fine.

5. Remove the culture from the incubator. Using fine forceps, move the coverslip to the imaging chamber and immediately cover with 1mL of the warm vehicle or experimental imaging solution. Make sure the cells are completely covered.
6. Transfer the cells to the microscope and scan for a healthy region of cells using DIC or brightfield microscopy under the 20× objective. Please refer to Fig. 2 for examples of healthy and unhealthy cells.
7. Obtain a DIC image of the selected imaging FOV using the optimized FOV size, location and binning previously determined in Section 4.3 steps 2 and 3, above. This will be used to generate cellular ROIs in the analysis.

This image must be taken at the exact same spatial resolution and imaging FOV size as the voltage imaging recordings.

8. Focus your cells in low-intensity red light before data acquisition. This will be slightly different from the DIC images focus point. Confirm cell health by noting the dye location. In healthy cells, the dye will localize to the extracellular surface creating a halo while unhealthy cells will show internalized dye in the cytosol. Please refer to Fig. 2 for examples of dye internalization.
9. Switch to a higher intensity and record two 10s videos at 500Hz.
10. This process can be repeated across multiple, separate fields on the same coverslip (we typically collect 4). Be sure to move each time to a new area

to prevent over exposure of the cells to light. If the cells have been overexposed, the firing frequency will decrease from one video to the next across all cells.

11. Repeat steps 1–9 for the remaining coverslips under your perturbation and control conditions.
12. When the acquisition is complete, export all of your data as .tiff files for analysis.

Organize the data into separate folders for each FOV containing the DIC image and voltage recording videos. This will expedite the analysis process significantly.

5. Analysis and interpretation of functional imaging data

5.1 Materials

Computer

External hard drive

Image analysis software (for example, MATLAB or ImageJ)

5.2 Analysis pipeline

1. Import voltage imaging data into an image analysis software system (ImageJ, for example). Custom imaging routines specifically designed for extracting voltage imaging data are available upon request from the authors.
2. Using the DIC image as a guide, create regions of interest (ROIs) over the cells of interest.
3. Plot the fluorescence gray values in these ROIs vs. time (see Fig. 3D).
4. To determine the firing frequency, count the number of spikes within the recording window (in this example, 10s).

5.3 Representation and interpretation of data

Voltage imaging data can provide a snapshot of the activity with a neuronal culture. In particular, the enhanced temporal resolution of voltage imaging with BeRST allows interrogation of changes in firing frequency—difficult or impossible to do with traditional Ca^{2+} imaging. Spike frequencies can be represented in a multitude of ways which can offer unique perspectives on the spiking activity under perturbed and unperturbed conditions. For example, in neurons treated with βHB , we see an overall decrease in the average firing rate compared to neurons maintained in glucose solution (Fig. 4A). Examining the activity data as a cumulative frequency plot reveals that the greatest changes in firing frequency take place in cells with relatively lower intrinsic firing rates (<2Hz or so), suggesting that the effects of βHB may be primarily isolated to excitatory, rather than inhibitory, neuronal subtypes (Fig. 4B).

6. Summary

In this chapter, we outlined a protocol for the use of Berkeley Red Sensor of Transmembrane potential (BeRST 1) in cultured neurons isolated from the hippocampus. The use of BeRST 1—and Voltage-sensitive Fluorophores, or VoltageFluors, more generally—enables rapid assessment of neuronal activity using readily available, commercial cameras, illumination sources, and microscope optics. We envision that BeRST 1 and related indicators will be of use in a number of applications, and we hope this chapter provides a starting point for others to perform voltage imaging measurements in their own laboratories.

7. Solutions

Use sterile double distilled water in all recipes and protocol steps.

Culture media (MEM++++)

10mL B27 (Invitrogen 17504-044)

5mL GlutaMAX (Invitrogen 35050-061)

25mL fetal bovine serum (VWR 89510-186)

10mL 1M dextrose (FischerScientific D16-500; sterile filtered)

500mL Media, MEM, for rat dissection (Invitrogen 11090-081)

Combine all components, sterile filter, and aliquot into 50mL tubes.

Store at 4°C for up to 6 months

Brain Phys media (BP+)

10mL NeuroCult SM1 (Stem Cell 05711)

5mL GlutaMAX (Invitrogen 35050-061)

500mL Media, BrainPhys (Stem Cell 05790)

Combine all components, sterile filter, and aliquot into 50mL tubes.

Store at 4°C for up to 6 months

Neurobasal media (NB++)

10mL B27 (Invitrogen 17504-044)

5mL GlutaMAX (Invitrogen 35050-061)

500mL Media, Neurobasal (Invitrogen 21103-049)

Combine all components, sterile filter, and aliquot into 50mL tubes.

Store at 4°C for up to 6 months

Sodium borate buffer

1.55g boric acid

4.50g sodium tetraborate decahydrate

500mL sterile double distilled water

Combine all components, bring the pH to 8.5, and sterile filter. Store at room temperature indefinitely

Metabolic salt solution

135.43mM sodium chloride.

5.33mM potassium chloride

4.17mM sodium bicarbonate

2.5mM D-glucose

1.25mM calcium chloride

0.49mM magnesium chloride

0.41mM magnesium sulfate

0.44mM potassium phosphate monobasic

0.34mM sodium phosphate dibasic

290mOsmols

Combine all materials, bring the pH to 7.3, measure osmolarity, sterile filter and store at 4°C

Acknowledgment

This work was supported in part by NSF 1707350. M.J.K. was supported in part by a training grant from NIH (5T32GM007232).

References

- Abdelfattah AS, Kawashima T, Singh A, Novak O, Liu H, Shuai Y, et al. (2019). Bright and photostable chemigenetic indicators for extended in vivo voltage imaging. *Science*, 365(6454), 699–704. 10.1126/science.aav6416. [PubMed: 31371562]
- Audesirk G, Audesirk T, & Ferguson C (2000). Culturing rat hippocampal neurons. *Current Protocols in Toxicology*, 4(1), 12.13.11–12.13.17. 10.1002/0471140856.tx1203s04.
- Bardy C, van den Hurk M, Eames T, Marchand C, Hernandez RV, Kellogg M, et al. (2015). Neuronal medium that supports basic synaptic functions and activity of human neurons in vitro. *Proceedings of the National Academy of Sciences of the United States of America*, 112(20), E2725–E2734. 10.1073/pnas.1504393112. [PubMed: 25870293]

- Braubach O, Cohen LB, & Choi Y (2015). Historical overview and general methods of membrane potential imaging. *Advances in Experimental Medicine and Biology*, 859, 3–26. 10.1007/978-3-319-17641-3_1. [PubMed: 26238047]
- Chen T-W, Wardill TJ, Sun Y, Pulver SR, Renninger SL, Baohan A, et al. (2013). Ultrasensitive fluorescent proteins for imaging neuronal activity. *Nature*, 499(7458), 295–300. 10.1038/nature12354. [PubMed: 23868258]
- Craven D, McGinley B, Kilmartin L, Glavin M, & Jones E (2015). Compressed sensing for bioelectric signals: A review. *IEEE Journal of Biomedical and Health Informatics*, 19(2), 529–540. 10.1109/JBHI.2014.2327194. [PubMed: 24879647]
- Deal PE, Liu P, Al-Abdullatif SH, Muller VR, Shamardani K, Adesnik H, et al. (2020). Covalently tethered rhodamine voltage reporters for high speed functional imaging in brain tissue. *Journal of the American Chemical Society*, 142(1), 614–622. 10.1021/jacs.9b12265. [PubMed: 31829585]
- Huang YL, Walker AS, & Miller EW (2015). A photostable silicon rhodamine platform for optical voltage sensing. *Journal of the American Chemical Society*, 137(33), 10767–10776. 10.1021/jacs.5b06644. [PubMed: 26237573]
- Kawamura MJ, Ruskin DN, & Masino SA (2016). Metabolic therapy for temporal lobe epilepsy in a dish: Investigating mechanisms of ketogenic diet using electrophysiological recordings in hippocampal slices. *Frontiers in Molecular Neuroscience*, 9, 112. 10.3389/fnmol.2016.00112. [PubMed: 27847463]
- Kazempour A, Novak O, Flickinger D, Marvin JS, Abdelfattah AS, King J, et al. (2019). Kiloherz frame-rate two-photon tomography. *Nature Methods*, 16(8), 778–786. 10.1038/s41592-019-0493-9. [PubMed: 31363222]
- Kulkarni RU, & Miller EW (2017). Voltage imaging: Pitfalls and potential. *Biochemistry*, 56(39), 5171–5177. 10.1021/acs.biochem.7b00490. [PubMed: 28745864]
- Lin MZ, & Schnitzer MJ (2016). Genetically encoded indicators of neuronal activity. *Nature Neuroscience*, 19(9), 1142–1153. 10.1038/nn.4359. [PubMed: 27571193]
- Liu P, & Miller EW (2020). Electrophysiology, unplugged: Imaging membrane potential with fluorescent indicators. *Accounts of Chemical Research*, 53(1), 11–19. 10.1021/acs.accounts.9b00514. [PubMed: 31834772]
- Ma W, Berg J, & Yellen G (2007). Ketogenic diet metabolites reduce firing in central neurons by opening K(ATP) channels. *The Journal of Neuroscience*, 27(14), 3618–3625. 10.1523/jneurosci.0132-07.2007. [PubMed: 17409226]
- Miller EW, Lin JY, Frady EP, Steinbach PA, Kristan WB Jr., & Tsien RY (2012). Optically monitoring voltage in neurons by photo-induced electron transfer through molecular wires. *Proceedings of the National Academy of Sciences of the United States of America*, 109(6), 2114–2119. 10.1073/pnas.1120694109. [PubMed: 22308458]
- Ortiz G, Liu P, Naing SHH, Muller VR, & Miller EW (2019). Synthesis of sulfonated carbofluoresceins for voltage imaging. *Journal of the American Chemical Society*, 141(16), 6631–6638. 10.1021/jacs.9b01261. [PubMed: 30978010]
- Pine J (2006). A history of MEA development. In Taketani M & Baudry M (Eds.), *Advances in network electrophysiology: Using multi-electrode arrays* (pp. 3–23). Boston, MA: Springer US.
- Roeper BLJ (2001). Molecular physiology of neuronal K-ATP channels. *Molecular Membrane Biology*, 18(2), 117–127. 10.1080/09687680110047373. [PubMed: 11463204]
- Sada N, Lee S, Katsu T, Otsuki T, & Inoue T (2015). Targeting LDH enzymes with a stiripentol analog to treat epilepsy. *Science*, 347(6228), 1362–1367. 10.1126/science.aaa1299. [PubMed: 25792327]
- Scanziani M, & Häusser M (2009). Electrophysiology in the age of light. *Nature*, 461(7266), 930–939. 10.1038/nature08540. [PubMed: 19829373]
- Sjulson L, & Miesenböck G (2007). Optical recording of action potentials and other discrete physiological events: A perspective from signal detection theory. *Physiology*, 22(1), 47–55. 10.1152/physiol.00036.2006. [PubMed: 17289930]
- Sofroniew NJ, Flickinger D, King J, & Svoboda K (2016). A large field of view two-photon mesoscope with subcellular resolution for in vivo imaging. *eLife*, 5, e14472. 10.7554/eLife.14472. [PubMed: 27300105]

- Tomina Y, & Wagenaar DA (2017). A double-sided microscope to realize whole-ganglion imaging of membrane potential in the medicinal leech. *eLife*, 6, e29839. 10.7554/eLife.29839. [PubMed: 28944754]
- Wu J, Liang Y, Chen S, Hsu C-L, Chavarha M, Evans SW, et al. (2020). KiloHertz two-photon fluorescence microscopy imaging of neural activity in vivo. *Nature Methods*, 17(3), 287–290. 10.1038/s41592-020-0762-7. [PubMed: 32123392]

Author Manuscript

Author Manuscript

Author Manuscript

Author Manuscript

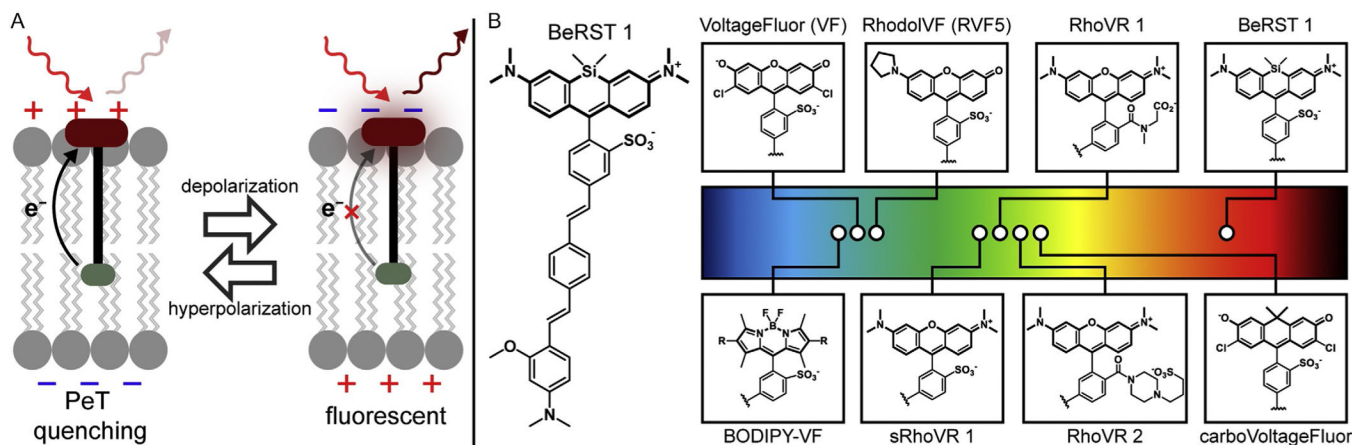


Fig. 1. Voltage-sensitive fluorophores sense membrane potential via photoinduced electron transfer (PeT). (A) Proposed mechanism of voltage sensing via PeT. At rest, electron transfer from an electron-rich aniline (green) to the fluorophore (red) quenches fluorescence. Upon depolarization of the plasma membrane, the transmembrane potential inhibits electron transfer, and fluorescence increases. (B) (*left*) The structure of BeRST 1 and (*right*) other Voltage-sensitive Fluorophores (VoltageFluors). The location of the circle in the rainbow spectrum indicates the approximate excitation wavelength required for the dye. Abbreviations: RhoVR, Rhodamine Voltage Reporter; BeRST, Berkeley Red Sensor of Transmembrane potential. sRhoVR is sulfonated RhoVR. *Adapted with permission from Acc. Chem. Res. 2020, 53, 11–19. Copyright 2020 American Chemical Society.*

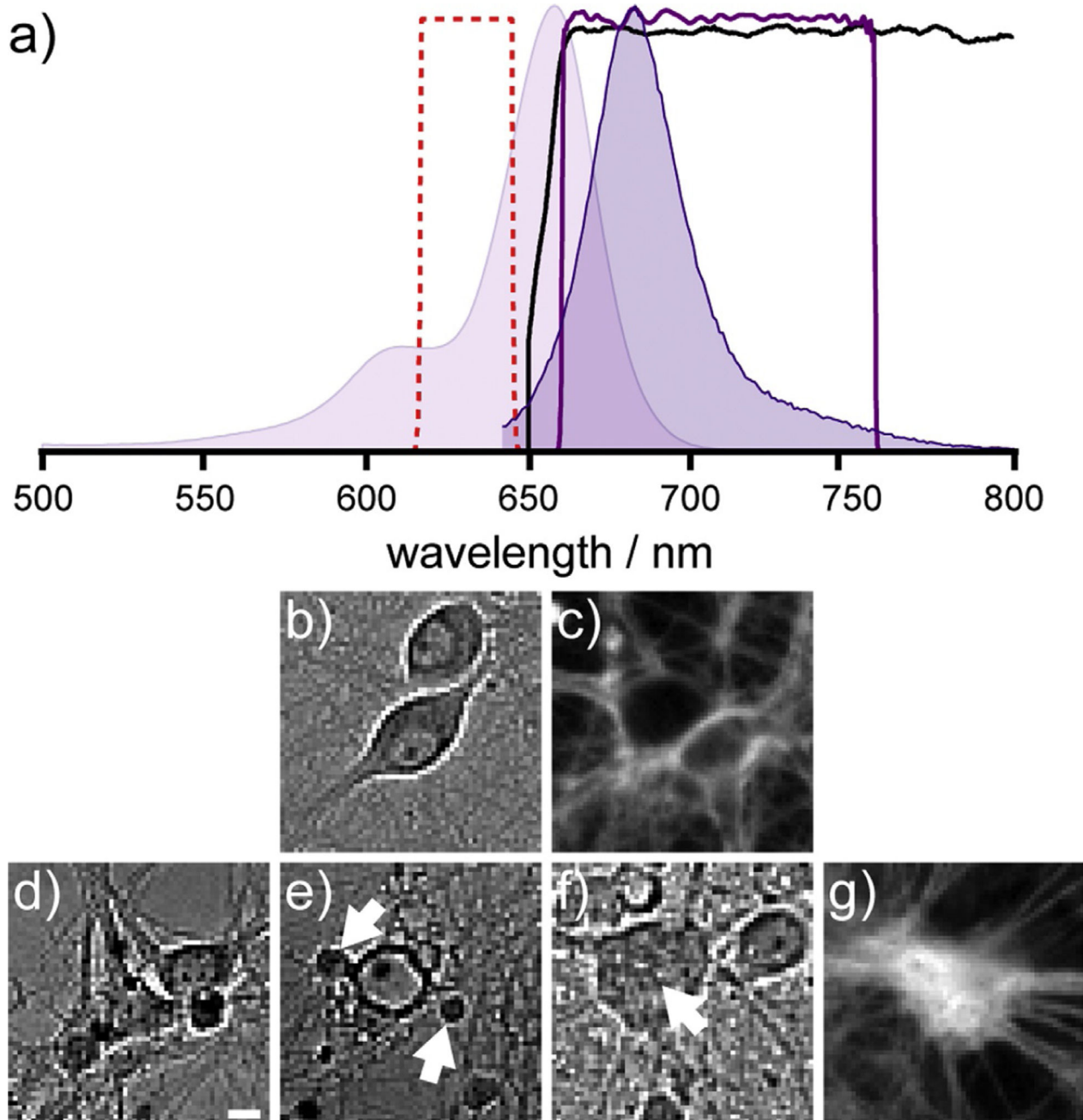


Fig. 2. Evaluating optics and cellular health for voltage imaging with BeRST 1. (A) Graphical representation of absorption (light purple) and emission (dark purple) spectra for BeRST 1. Overlaid are the excitation band from the LED light source (red), dichroic mirror (black) and emission bandpass filter (dark purple line). (B and C) Example of healthy hippocampal neurons. (B) Representative DIC image of healthy hippocampal neurons, with robust halos around their membranes, no blebbing, and clear nuclear compartments. (C) Representative epifluorescence micrograph of healthy neurons in which BeRST 1 is localized to the extracellular surface, forming a halo-like structure around each cell body. (D–G) Examples

of unhealthy neurons. (D) DIC micrograph of cells forming a neurosphere structure, where cells overlap significantly in a central sphere and projections radiate outward. This structure indicates unhealthy neurons. (E) DIC micrograph of blebbing of a cell membrane. The membrane of the large, central cell shows a large amount of deterioration, forming bubbles or blebs at the surface of the cell, indicated by the white arrow. (F) DIC micrograph of a single large cell with no defined nucleus. The expected location of the nuclear membrane is indicated by the white arrow. (G) Epifluorescence image of an unhealthy neurosphere structure which has taken up dye molecules and is thus fluorescent throughout the intracellular space. Scale bar is 10 μ m.

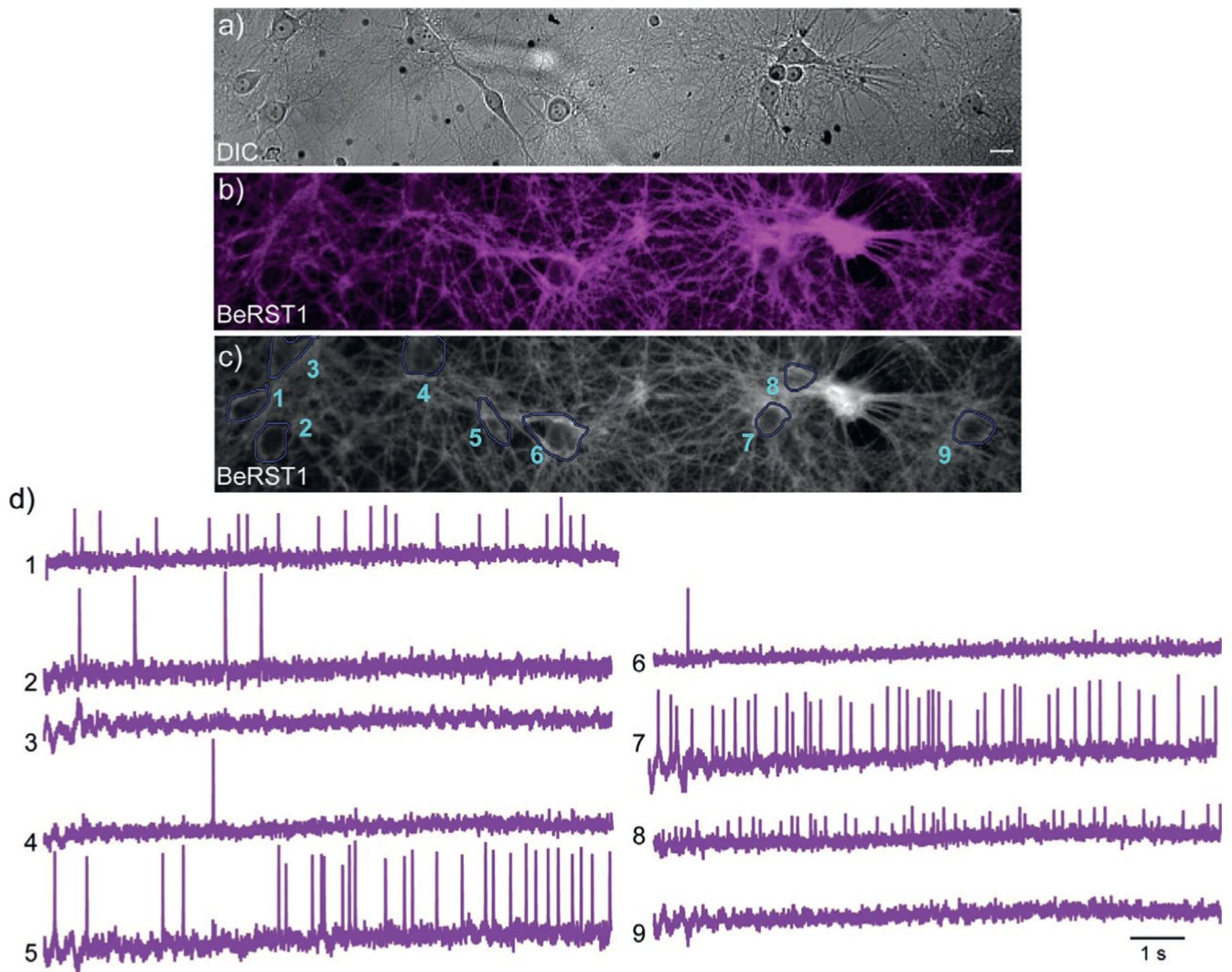


Fig. 3. Example data from a single 10s recording of 10 dissociated neurons in culture as reported by BeRST 1. (A) DIC micrograph of 512×100 imaging field of view (FOV) region showing 10 healthy cell bodies. Scale bar is $20\mu\text{m}$. (B) Fluorescent microscopy image of the same 512×100 imaging FOV stained with 500nM BeRST1. (C) Fluorescent micrograph showing selected cellular ROI for analysis. (D) Representative fractional change in fluorescence (F/F) traces extracted from the 10s video of cellular ROIs 1–10. Here each trace represents the fluorescent responses indicated cell from panel (C) as reported by BeRST1.

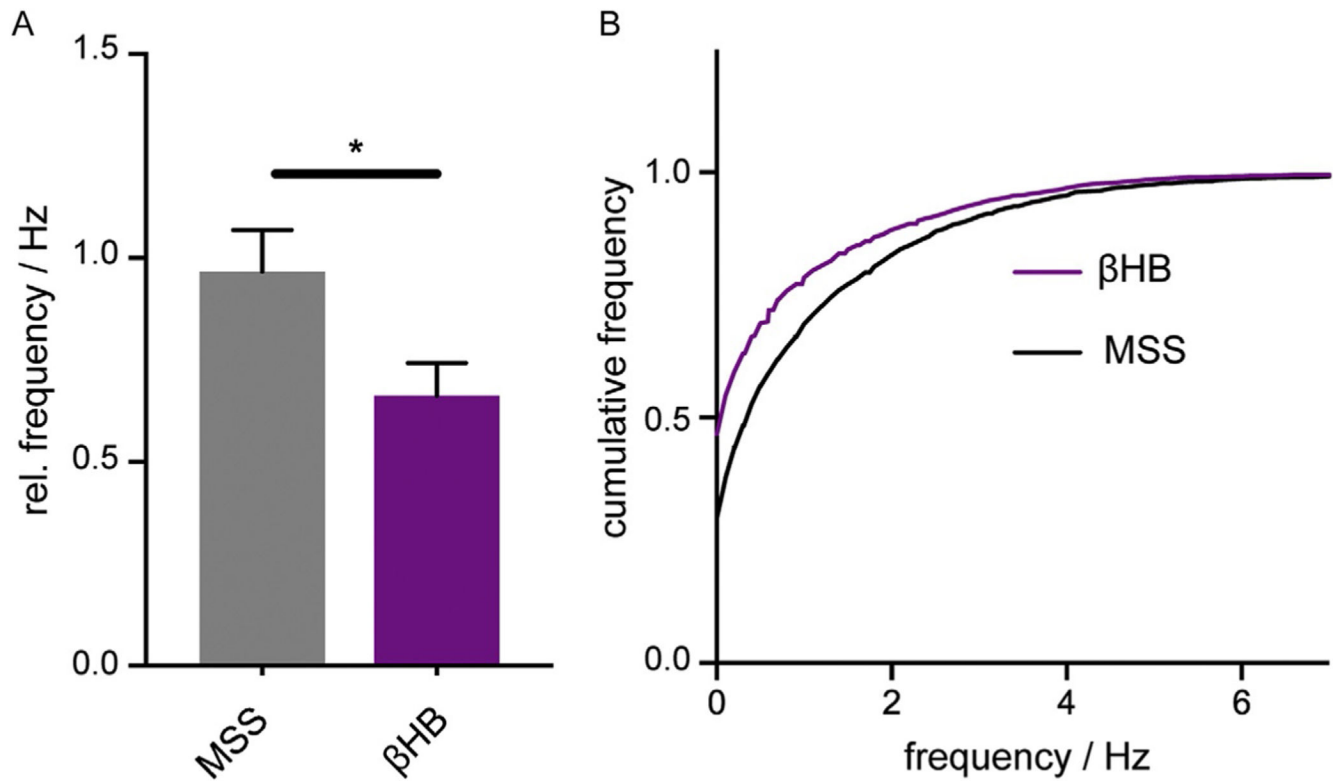


Fig. 4. Representative data set showing a comparison of spike frequency differences under glucose-treated and β -hydroxybutyrate (β HB) treated conditions. (A) Bar graph depicting mean firing frequency across $n = 43$ coverslips of neurons for β HB and $n=36$ coverslips for glucose (error bars are standard error of the mean, Mann Whitney test * is $P=0.0142$). (B) Cumulative frequency distribution of single cell frequencies under β HB- and glucose-treated conditions.